

2017

Relating Nanoscale Accessibility within Plant Cell Walls to Improved Enzyme Hydrolysis Yields in Corn Stover Subjected to Diverse Pretreatments

Jacob D. Crowe
Michigan State University

Rachael A. Zarger
Michigan State University

David B. Hodge
Luleå University of Technology, hodgeda@msu.edu

Follow this and additional works at: <https://digitalcommons.unl.edu/usdoepub>

Crowe, Jacob D.; Zarger, Rachael A.; and Hodge, David B., "Relating Nanoscale Accessibility within Plant Cell Walls to Improved Enzyme Hydrolysis Yields in Corn Stover Subjected to Diverse Pretreatments" (2017). *US Department of Energy Publications*. 371.
<https://digitalcommons.unl.edu/usdoepub/371>

This Article is brought to you for free and open access by the U.S. Department of Energy at DigitalCommons@University of Nebraska - Lincoln. It has been accepted for inclusion in US Department of Energy Publications by an authorized administrator of DigitalCommons@University of Nebraska - Lincoln.

Relating Nanoscale Accessibility within Plant Cell Walls to Improved Enzyme Hydrolysis Yields in Corn Stover Subjected to Diverse Pretreatments

Jacob D. Crowe,[†] Rachael A. Zarger,[†] and David B. Hodge^{*,†,‡,§,||}

[†]Department of Chemical Engineering and Materials Science, [‡]DOE-Great Lakes Bioenergy Research Center, and [§]Department of Biosystems & Agricultural Engineering, Michigan State University, East Lansing, Michigan 48824, United States

^{||}Department of Civil, Environmental and Natural Resources Engineering, Luleå University of Technology, Luleå 97187, Sweden

ABSTRACT: Simultaneous chemical modification and physical reorganization of plant cell walls via alkaline hydrogen peroxide or liquid hot water pretreatment can alter cell wall structural properties impacting nanoscale porosity. Nanoscale porosity was characterized using solute exclusion to assess accessible pore volumes, water retention value as a proxy for accessible water–cell walls surface area, and solute-induced cell wall swelling to measure cell wall rigidity. Key findings concluded that delignification by alkaline hydrogen peroxide pretreatment decreased cell wall rigidity and that the subsequent cell wall swelling resulted increased nanoscale porosity and improved enzyme binding and hydrolysis compared to limited swelling and increased accessible surface areas observed in liquid hot water pretreated biomass. The volume accessible to a 90 Å dextran probe within the cell wall was found to be correlated to both enzyme binding and glucose hydrolysis yields, indicating cell wall porosity is a key contributor to effective hydrolysis yields.

KEYWORDS: lignocellulosic biomass, cell wall properties, nanoscale porosity, alkaline hydrogen peroxide (AHP) pretreatment, liquid hot water (LHW) pretreatment, enzymatic hydrolysis

■ INTRODUCTION

Lignocellulosic biomass is a promising feedstock for the production of renewable fuels and chemicals. One key challenge limiting effective utilization of biomass resides in plant-evolved cell wall recalcitrance¹ or resistance to degradation imparted by the higher-order structure of plant cell walls. The physical structure of the plant cell wall matrix can be considered a nanostructured composite material, with networks of cellulose fibril bundles and matrix polymers forming cell wall layers.² Networks of microfibrils are associated and potentially cross-linked with amorphous hemicellulose polysaccharides through noncovalent interactions.³ In lignified secondary cell walls, this network can contain lignin, which is deposited to impart structural rigidity, reduce water and solute permeability, and limit extracellular interactions.⁴ While containing similar major cell wall components, monocots and dicots contain different abundances and substitutions of hemicelluloses,³ as well as variations in lignin composition, abundance, and structure.⁴ As a unique feature to grass cell walls, the presence of hydroxycinnamates, specifically *p*-coumarate and ferulate can account for a nontrivial fraction of lignin composition.⁵ Ferulates have the capacity to dimerize, as well as form ferulate ester cross-links to xylans, resulting in xylan-lignin covalent linkages that have been hypothesized to contribute to cell wall recalcitrance in developing tissues as well as certain anatomical fractions.⁶

Thermochemical pretreatment can be applied to improve the deconstruction of plant cell wall polysaccharides by cellulolytic enzymes,⁷ with the goals of pretreatment to reduce recalcitrance by removing or redistributing hemicellulose and lignin, disrupting the crystalline structure of cellulose, or

disrupting the cell wall ultrastructure. Pretreatments often have the net effect of increasing cellulose accessibility to cellulolytic enzymes.⁸

While cellulose accessibility can be considered as the ability for an enzyme to bind to cellulose and hydrolyze a glycosidic bond, this property is often indirectly assessed as accessible surface area defined by a combination of particle size, porosity, and pore volume.⁹ Porosity in the context of the plant cell wall matrix can be due to a combination of composition and structural features impacting the rigidity and internal surface area of the composite polymer network. Lignin is a hydrophobic component when sufficiently removed from the cell wall, has been directly associated with loss of cell wall rigidity.¹⁰ Xylan removal is also associated with increases in cell wall porosity, however is coupled to a certain level of lignin removal depending on pretreatment.¹¹ Removal or relocalization of cell wall components alters the structural integrity of the cell wall matrix, allowing swelling and contraction in response to the solvent, exhibiting behavior similar to a hydrogel. It is with this model in mind that porosity is a dynamic term that defines both structural features and cell wall response to environmental conditions.

Techniques that measure properties of porosity often measure bulk property metrics of the cell wall such as water–cell wall associations using the water retention value (WRV),¹² measuring cell wall surface adsorption with dyes of known

Received: July 14, 2017

Revised: August 29, 2017

Accepted: September 6, 2017

Published: September 6, 2017

hydrodynamic radii to determine accessible substrate area using the Simons' Stain technique¹³ or of fluorescent-labeled enzymes for direct enzyme accessibility measurements.¹⁴ Water constraint measured using T₂ NMR relaxometry provides information on the extent of water–cell wall hydrogen bonding, with increased water constraint associated with increased water accessibility within the cell wall.¹⁵ Pore volume is a specific characteristic of porosity, defined by the porous nature of the cell wall in an idealized slit model. In the idealized slit model, the cell wall is thought of as a series of variably spaced lamellae that contain distinct pore size and therefore pore volume characteristics.¹⁶ The effect of cell wall component removal or relocalization during pretreatment can be associated with changes in the cell wall ultrastructure inducing 3D topographical changes in the form of induction of pore formation or voids.¹⁷ Techniques to measure cell wall pore distributions quantify the interaction of water within the pores to determine pore distributions. Solute exclusion utilizes the availability of porous water to influence diffusion of a probe of a known hydrodynamic radii into a pore of equal or larger diameter,¹⁶ however, is dependent upon uniform pore sizes for accurate pore volume determination.¹⁸ Differential scanning calorimetry-thermoporometry quantifies heat endotherms associated with freezing point depression of water closely associated with an interface,¹⁹ whereas ¹H NMR cryoporosimetry quantifies water content through similar thermochemical assumptions.²⁰ However, cryoporosimetry requires assumed pore geometries to extract meaningful pore distributions.

The relationship between pore volume and enzymatic hydrolysis has been investigated in multiple studies. Originally observed as differences in the initial rates of glucose hydrolysis for acid-pretreated hardwoods and softwoods,²¹ a positive correlation between pore volume and enzymatic hydrolysis has also been determined in other pretreatment and feedstock systems such as chlorite-delignified sugar cane bagasse.²² Other studies have not observed similar trends, with dilute acid pretreatment of corn stover showing no discernible relationship between pretreatment severity, hydrolysis yield, and pore volume.²⁰ Different methods of measuring pore properties such as Simons' Stain coupled with differential scanning calorimetry-thermoporometry have been recently used to evaluate alkali, autohydrolysis, and multistage pretreatments of wheat straw, concluding that delignification increases pore accessibility, while autohydrolysis increased cellulose accessibility at the expense of restricted pore accessibility.²³ Our prior work has also demonstrated relationships between water sorption, water retention, and settling volume as predictors for enzyme binding and enzymatic hydrolysis using alkaline hydrogen peroxide and liquid hot water pretreatment of corn stover and switchgrass.¹²

The goals of this study are to investigate corn stover subjected to a range of pretreatment conditions that include alkaline hydrogen peroxide (AHP) delignification and liquid hot water (LHW) pretreatment. These pretreatment-modified feedstocks are used to assess the impact of pretreatment on cell wall structural properties and to highlight key relationships between cell wall properties and enzymatic hydrolysis. The role of nanoscale porosity as a key structural property is investigated in the context of both solute exclusion measured accessible pore volumes, WRV-determined accessible water–cell wall surface area, and solute-induced cell wall swelling. Correlations derived from both these chemical and physical changes in the cell wall are developed and these properties are then related to

enzyme accessibility and enzymatic hydrolysis of cell wall polysaccharides.

METHODS AND MATERIALS

Biomass and Composition Analysis. Corn stover (*Zea mays* L. Pioneer hybrid 36H56) harvested in 2012 was milled with a Wiley Mini-mill (Thomas Scientific) to pass a 5 mm screen and air-dried to a moisture content of approximately 5% prior to any pretreatments. Milled material was sieved, and a particle size distribution between 425 μ m and 1 mm was selected for use in all pretreatments and subsequent experiments. Cell wall lignocellulosic material was isolated following the extraction and destarching procedure outlined by Foster et al.,²⁴ including three sequential washes of 70% ethanol, 1:1 methanol-chloroform, and acetone to obtain alcohol insoluble residue (AIR). AIR was destarched using 50 μ g Amylase/mL H₂O (*Bacillus* sp., Catalog # A7595, Sigma-Aldrich St. Louis, MO) and 18.7 units of Pullulanase (*Bacillus acidopullulyticus*, Catalog # P9286 Sigma-Aldrich, St. Louis, MO) in a 0.01% sodium azide solution, with rotary mixing (Intelli-Mixer, ELMI-tech, Newbury Park, CA) at 37 °C overnight. The noncellulosic neutral monosaccharide content of the wall matrix polysaccharides was determined following trifluoroacetic acid (TFA) hydrolysis of the destarched AIR followed by derivatization of the monosaccharides as alditol acetate method by GC/MS according to Foster et al.²⁴ Lignin content was determined on AIR biomass using the NREL/TP 510-42618 protocol.²⁵ Composition analysis was performed in technical triplicate.

Pretreatments. AHP pretreatment was performed using four different H₂O₂ to biomass loadings, 0, 0.06, 0.12, and 0.25 g H₂O₂/g biomass, at an insoluble solid loading of 15% (mass biomass per total liquid volume). Samples were prepared in 250 mL Erlenmeyer flasks, sealed with parafilm to allow expansion due to O₂ evolution, and placed in an incubator at 30 °C with shaking at 180 rpm for 24 h. The pH was maintained at 11.5 during pretreatment, with adjustments at 3 and 6 h using 3 M NaOH.¹² LHW pretreatments were performed in a 5 L M/K Systems digester (M/K Systems, Inc., Peabody, MA, U.S.A.). Using 100 mL pressure tubes (Ace Glass, Sigma-Aldrich, St. Louis, MO), 6.0 g of biomass was loaded with 70 mL of deionized water, yielding a solids content of 8.5% (mass biomass per total liquid volume). Pretreatment conditions were specified at either 160 °C for 30 min or 190 °C for 5 min, with a heat-up rate of 1.0 °C/min and a cool-down rate of approximately 1.0 °C/min. All biomass following pretreatment was washed until clear, vacuum filtered with a 200 mesh Buchner filter to a moisture content of approximately 85% measured gravimetrically, and stored at 4 °C. AHP pretreatment on LHW-pretreated material for two-stage pretreatments was performed under identical conditions as described previously, using thoroughly washed LHW pretreated material dried to a moisture content of about 5% and sieved to ensure similar particle sizes as the initial AIR material. Material drying for hornification measurements was performed in a temperature-controlled oven (Isotemp, Fisher Scientific) at 105 °C.

Enzymatic Hydrolysis. Enzymatic hydrolysis was performed on never-dried pretreated material in 250 mL Erlenmeyer flasks using 5% (insoluble mass biomass per total liquid volume) dry solids loading with the moisture content of the never-dried material determined separately to achieve the target solids loading. Reaction media was buffered pH 5.2 using 50 mM sodium citrate buffer, with pH adjustments occurring after 6-h and 24-h hydrolysis times. Tetracycline and cycloheximide at a total concentration of 40 μ g/mL each were used as antimicrobials during hydrolysis. Enzyme loading was performed using Cellic CTec3 and HTec3 (Novozymes A/S, Bagsværd, Denmark) at 20 mg protein/g glucan for CTec3 loading, and 10 mg protein/g glucan for HTec3 loading when HTec3 was added. Hydrolysis was performed at 50 °C with orbital shaking at 180 rpm and sampling was taken at 6-h and 72-h total hydrolysis times to represent short-term hydrolysis yields (6-h) and complete depolymerization yields (72-h). Samples were centrifuged at 13000g for 2 min postincubation and filtered using 22 μ m mixed cellulose-ester filters (EMD Millipore, Billerica, MA). Samples were quantified by HPLC (Agilent 1100 Series) equipped with an Aminex HPX-87H

column (Bio-Rad, Hercules, CA, U.S.A.) using a mobile phase of 5 mM H₂SO₄ at 65 °C. Glucose yields were determined based on quantified glucose (as glucan) relative to total glucan available, including noncellulosic glucan. All hydrolysis runs were performed in technical triplicate.

Water Retention Value. Water retention values (WRVs) were determined according to a modified version of TAPPI UM 256, as previously described,¹² with a centrifuge speed of 4000g for 15 min. Briefly, approximately 2.5 g of wet prewashed biomass samples were soaked in about 150 mL of either deionized water, or one of four NaCl solutions (0.25, 0.5, 0.75, and 1.0 M). After soaking for 1 h, samples were rinsed with around 200 mL of deionized water to remove salts and vacuum filtered using a 200-mesh Buchner filter. Washed biomass was inserted into a spin-column (Handee Spin Column Cs4, Thermo Scientific) with a 200-mesh stainless steel membrane. Biomass was added to form a circular cake devoid of large spaces, with care taken to avoid inducing drainage of biomass from pressing into column. Nonbound water was drained via centrifugation at 4000g for 15 min. The mass of the drained biomass was determined using tared aluminum trays, and dried in an oven at 105 °C for at least 3 h, then weighed again. The WRV was determined as the ratio of the mass of water remaining in the biomass after centrifuging divided by the mass of dry biomass. WRV was determined in technical triplicate.

Solute Exclusion. Solute exclusion was performed following the original protocol outlined by Stone and Scallan,²⁶ using a series of neutral dextran probes of increasing molecular weight, with some minor modifications to the procedure. Table 1 lists the probes used in

Table 1. Neutral Dextran Probes Used in Solute Exclusion Technique

probe molecules	mol. mass ^a (Da)	mol. diameter ^b (Å)
D-(+)-Cellobiose	342	8
Dextran 6k	6000	39
Dextran 40k	40000	90
Dextran 70k	70000	110
Dextran 100k	100000	136
Dextran 450–650k	550000	310
Dextran 2000k	2000000	560

^aFrom the manufacturer. ^bInterpolated from Stone and Scallan.¹⁵

this study, which were obtained from Sigma-Aldrich. For this, approximately 5.0 g of wet, or 1.0 g of oven-dried biomass was added to tared 50 mL centrifuge tubes and reweighed after biomass

addition. About 10 mL 0.4% (w/v) dextran solution by was added to each tube, and reweighed. Tubes were vortexed for thorough mixing, stored at 4 °C for 48 h, and periodically vortexed for the duration of probe-biomass mixing. A 1 mL sample was taken, centrifuged at 13 000g for 2 min, and transferred to a sealed vial for HPLC (Agilent 1100 Series) analysis. Biomass solids were thoroughly washed to remove the dextran probes in centrifuge tubes through dilution with water followed by centrifugation and solid–liquid separation, which was repeated three times. Centrifugation was performed at 900g for 3 min, with washed biomass dried overnight in a 105 °C oven to determine oven dry biomass weight. Probe concentration was quantified using refractive index on the HPLC, with no column attached as described previously.²⁰ Blanks were used to determine any background or nondextran probe contributions to the refractive index signal. Inaccessible pore volume was determined as previously outlined.¹⁸ Samples were performed in technical triplicate.

Enzyme Binding. Enzyme-binding experiments were performed on never-dried biomass using 0.2 g biomass (dry basis)/ 10 mL solution buffer solution containing a cellulase cocktail (CelliC CTec3). Binding isotherms were determined for protein concentrations over a range of 0 to 3.0 mg/mL (protein content determined using nitrogen adsorption) in a 50 mM Na-citrate buffer solution at pH 5.2. Samples were mixed overnight at 4 °C using rotary mixing (Intelli-Mixer, ELMI-tech, Newbury Park, CA). Bound protein mass was determined from the difference between unbound protein in free solution to total initial protein concentration determined using the Bradford method.²⁷ Bound protein fraction was determined using a standard calibration curve of initial protein concentrations. Bound enzyme fractions were determined from linear fit of bound enzyme for the linear region of the Langmuir adsorption isotherm as described in our previous work.¹² Samples were performed in technical duplicate, with error associated with linear regression fitting determined.

RESULTS AND DISCUSSION

Composition Analysis and Enzymatic Hydrolysis.

Composition profiles of residual solids after AHP delignification, LHW pretreatment, and combinations of the two as shown in Figure 1. These conditions were selected to generate three distinct feedstock groups with significantly different residual solids compositions that exhibit a wide range of materials for properties testing. The results show that AHP-delignified biomass demonstrated a clear trend of increasing lignin removal with increasing H₂O₂ loading (Figure 1) while retaining most of the xylan as demonstrated in our previous

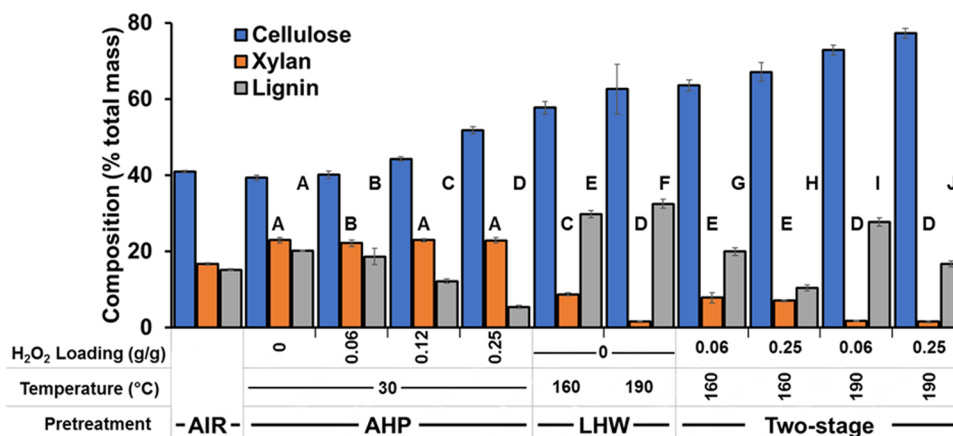


Figure 1. Compositional profiles of corn stover subjected to either AHP pretreatment, LHW, or LHW followed by AHP pretreatment. Compositional profiles for xylan, crystalline cellulose, and Klason lignin are shown for alcohol insoluble residue (AIR) corn stover and pretreated biomass. Composition analysis was performed in technical triplicate ($n = 3$), with standard deviations shown on figure. Statistical analysis was performed with Fisher Least Significant Difference (95% confidence) to determine individual statistical groupings (denoted as A, B, C, etc. above each bar) for both xylan and lignin contents individually between pretreatments.

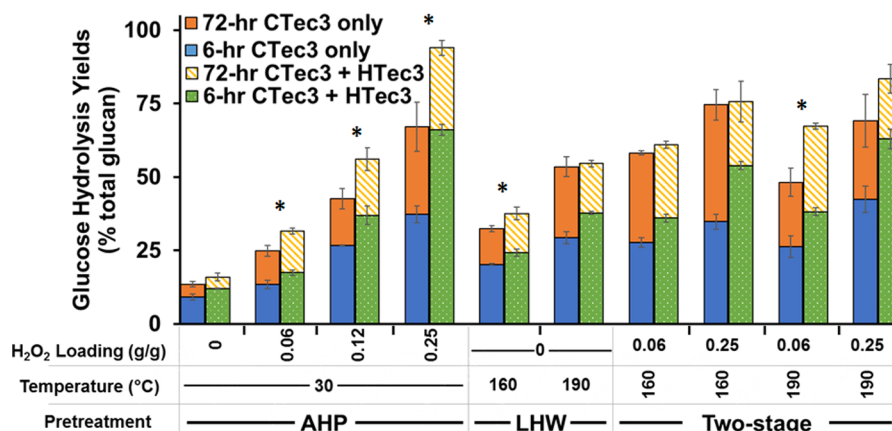


Figure 2. Enzymatic hydrolysis glucose yields of pretreated corn stover samples. Results of never-dried hydrolysis of pretreated samples for 6-h total hydrolysis time are plotted in blue and dotted green, while 72-h total hydrolysis times are plotted above in orange and striped gold. Solid bars represented hydrolysis conditions using only 20 mg protein/g glucan cellulase loading, while patterned bars represent hydrolysis conditions using both 20 mg protein/g glucan and 10 mg protein/g glucan hemicellulase loading. Analysis was performed in technical triplicate. * indicate statistical significance between 72-h CTec3 only and 72-h CTec3 + HTec3 for each pretreatment condition (Student's *t* test 95% confidence).

work.²⁸ The LHW-pretreated biomass showed significant xylan removal through solubilization, with the 160 °C condition containing about 8% residual xylan by mass, while the 190 °C LHW condition had near complete removal of xylan. Residual biomass was enriched in cellulose and lignin content for both conditions and was consistent with primarily xylan solubilization observed with corn stover LHW pretreatment.²⁹ The combination of LHW pretreatment followed by AHP delignification was performed at two AHP loadings (0.06 and 0.25 g H₂O₂/g biomass) for both LHW pretreatment conditions to generate pretreated feedstocks with modified xylan and lignin content. These pretreatment combinations represent a wide range of altered cell wall compositions, with cellulose accounting for up to 80% total mass for the most severe pretreatment condition (Figure 1). Interestingly, the lowest H₂O₂ loading for AHP delignification (0.06 H₂O₂/g biomass) for both LHW-pretreated biomass conditions resulted in significantly higher removal of lignin compared to the same AHP delignification conditions and may be due to lignin reallocation associated with LHW pretreatment above the glass-transition temperature increasing lignin accessibility to removal by AHP after LHW pretreatment.

Subsequent enzymatic hydrolysis was performed on never-dried pretreated biomass using either a cellulase cocktail (Cellic CTec3) or a combined cellulase/hemicellulase cocktail (CTec3 + HTec3) to measure the impact of cell wall composition and, indirectly, the modification of the higher-order structure of the cell wall matrix by pretreatment on the rate and extent of cellulose enzymatic hydrolysis. Results for 6-h and 72-h glucose hydrolysis yields, representing initial rate and final extent of hydrolysis respectively, are shown in Figure 2. These results show that enzymatic hydrolysis using a cellulase and hemicellulase cocktail on the AHP-only pretreated biomass resulted in high (94%) glucose hydrolysis yields at the highest H₂O₂ loading, while LHW-pretreated biomass achieved only a 54% glucose yield at the highest severity. Interestingly, a glucose yield of only 83% was observed for the highest severity two-stage pretreatment, which can be attributed to cell wall structural changes from the two-stage pretreatment limiting enzymatic hydrolysis. Reductions in cellulose accessibility resulting from cellulose aggregation induced by sufficient removal of noncellulosic components in the cell wall would

explain both reduced hydrolysis kinetics, as well as limited cellulose hydrolysis.³⁰

The cellulase enzyme cocktail used in this study (i.e., CTec3) has been shown to contain a suite of accessory enzymes including xylanase and pectinase activities.³¹ Furthermore, this cocktail is capable of effectively hydrolyzing pretreated biomass with low to moderate hemicellulose content without any additional accessory enzymes;³¹ however, significantly lower yields are observed in pretreated feedstocks containing a substantial fraction of the original xylan, such as the AHP-only samples.³² In the AHP-only case, delignification may increase enzymatic hydrolysis effectiveness; however, as reported in prior studies, cellulose accessibility is likely inhibited by both lignin and xylan content,³³ with lignin limiting accessibility to xylan-coated cellulose microfibrils. Therefore, for AHP-only pretreated biomass, we can hypothesize that without removal of xylan, significant regions of the cell wall matrix remain partially inaccessible to cellulase binding. This result is further exemplified by the similar yields observed between the cellulase only and cellulase plus hemicellulase for the 160 °C LHW two-stage pretreatments (Figure 2), which contain significantly lower xylan content compared to the AHP-only pretreatments. Enzymatic hydrolysis using only the cellulase cocktail also resulted in notable lower 6-h glucose hydrolysis yields for all samples, indicating that lack of xylanase and pectinase hinders initial hydrolytic rate of cellulases due to xylan limiting cellulose accessibility. It is noted however that 6-h glucose hydrolysis yields may be impacted by incomplete depolymerization of cellulose oligosaccharides in solution and cannot be deconvoluted in this study due to only quantification of glucose monomeric sugars. This conclusion is further supported by higher initial yields associated with highly delignified samples, with delignification acting as an alternative avenue to increase enzyme accessibility.³⁴

Nonproductive adsorption may also play a role in limiting enzymatic hydrolysis effectiveness, as there was a noted increase in enzymatic hydrolysis yields between the cellulase only and cellulase plus hemicellulase cases for the two-stage 190 °C LHW-pretreated biomass, as xylan content accounted for less than 2% of total cell wall mass. This result indicates higher overall enzyme loading may limit the effect of nonspecific binding of enzymes to lignin by providing more protein for

adsorption to the charged surface of lignin, effectively neutralizing the lignin surface and promoting cellulase adsorption to cellulose.

Cell Wall Swelling in Response to Increasing Solvent Ionic Strength. Water retention value is a property that can be used to capture a number of different structural features of the cell wall matrix as they relate to cell wall association with water. As demonstrated in our recent work, WRV can be used to predict enzymatic hydrolysis in two different alkaline pretreatments under a range of conditions,³⁵ with WRV able to capture higher-order changes in the cell wall associated with nanoscale porosity and cellulose accessibility in compositionally diverse pretreated samples. WRV is used similarly in this study to understand changes in higher-order structure; however, WRV are lower in this work due to changes in methodology increasing the amount of dewatering compared to prior work.¹² In the present work, the WRV without an added solute was found to increase with increasing H₂O₂ loading in the AHP-only pretreatment case, as well as increasing severity for LHW pretreatment (Figure 3). Increases in WRV were also observed

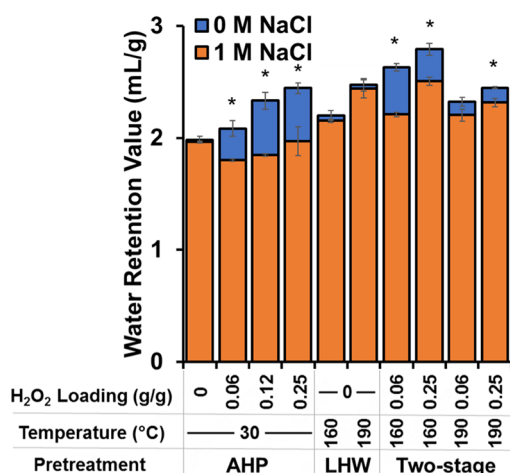


Figure 3. Cell wall swelling measured using water retention in the absence and presence of a salt. Water retention value (WRV) of never-dried corn stover at varying pretreatments measured after incubation in water only (blue bars) or 1 M NaCl (orange bars). Samples were performed in technical triplicate ($n = 3$), with standard deviation shown on figure. * indicates statistical significance between 0 M NaCl and 1 M NaCl for individual pretreatment conditions (Student's t test 95% confidence).

between low and high H₂O₂ loading for individual two-stage pretreatments. These results indicate delignification by AHP and xylan removal by LHW pretreatment can increase the amount of water associated with the cell wall matrix. A noted decrease in WRV in the 190 °C LHW two-stage pretreatments may be attributed to two contributions; the first suggesting delignification in low-xylan cell walls removes sufficient spacer components that could be hypothesized to result in cellulose aggregation and collapse of the cell wall matrix, limiting available sites for water entrapment. The second contribution may be due to lignin content making up a larger composition fraction of the 190 °C LHW two-stage pretreatments compared to the AHP-only and 160 °C LHW two-stage pretreatment, and subsequently limiting the amount of water associated with the cell wall.

The values for WRV in the presence of an added solute showed noted decreases for the high H₂O₂ loading AHP-only

samples, as well as 160 °C LHW two-stage pretreatments, while no decrease in WRV was observed in the 0 g/g H₂O₂ AHP-only sample or the LHW only samples. The impact of increasing solvent ionic strength on cell wall water retention has been investigated largely in the context of pulp and paper applications.³⁶ From our results, delignification appears to be the primary contributor to solute-induced changes in WRV and can be interpreted as a change in cell wall rigidity. Within the secondary cell walls of grasses, lignin forms a rigid matrix, with ferulate-mediated cross-links between within lignin and between lignin and xylans preventing physical cell wall expansion in response to the solvent environment.^{5,37} Lignin content within the cell wall correlates to the extent of enzymatic hydrolysis in grasses, with greater than 50% cell wall delignification associated with high (>80%) hydrolysis yields.¹⁰ Disruption of lignin structure through sufficient cleavage of cross-links and solubilization can be proposed to contribute to a loss of cell wall rigidity, allowing the cell wall to exhibit hydrogel-like behavior in the presence of solutes.

The equilibrium swelling of hydrogels is known to depend on factors that include the cross-link and charge densities of the polymer networks, while increases in the number of ionic groups in hydrogels can increase the swelling capacity by increasing osmotic pressure that driving the infiltration of solvent into the polymer network.³⁸ This behavior has been observed in carboxymethyl cellulose gels and to a lesser extent sulfite pulps, which exhibited changes in WRV corresponding roughly to the content of acidic groups.³⁶ AHP pretreatment has been shown to increase the cell wall carboxylate content,¹² which would explain the swelling behavior of AHP-delignified biomass, although solute-induced changes in WRVs are not as pronounced as prior work using chlorite-delignified pulps.³⁹ The extent of noncovalent physical association of cell wall components contributes to the ability of the cell wall to swell, as cell wall swelling is not as pronounced in the two-stage 190 °C LHW-pretreated biomass, which can be hypothesized to be due to partial cell wall coalescence.

Accessible Volume Distributions Determined by Solute Exclusion. A set of dextran probes was next employed to assess the accessible nanoscale volume within the pretreated biomass. Accessible volume distributions were determined by subtraction of inaccessible volumes from the inaccessible volume at the largest probe size (560 Å), representing the total volume for a sample.¹⁶ It should be noted that these volumes are not direct measurements of cell wall pores but rather effective pore diameter based upon idealized probe diameter in solution;⁴⁰ thus, they will be referred to as probe diameter in this work, as shown in Figure 4. From these results, there are clear differences in accessible volumes between AHP-only, LHW-only, and two-stage pretreatments. In the AHP-only samples, accessible volume was restricted to only smaller (<12 Å) probe sizes for the 0 g/g H₂O₂ pretreated sample, while increasing H₂O₂ loading resulted in significant increases in accessible volumes for both small and large probes, indicating the formation of larger (>39 Å) porous voids.¹⁶ Studies using chlorite-delignified sugarcane bagasse have yielded highly similar accessible volume distributions to the AHP-only pretreated samples in this work, indicating that delignification of diverse graminaceous biomass feedstocks results in similar cell wall responses and that lignin removal may result in the formation of water-accessible surfaces within the cell wall.²²

Accessible volume distributions in the LHW samples showed some noted increases in accessible volumes for probes between

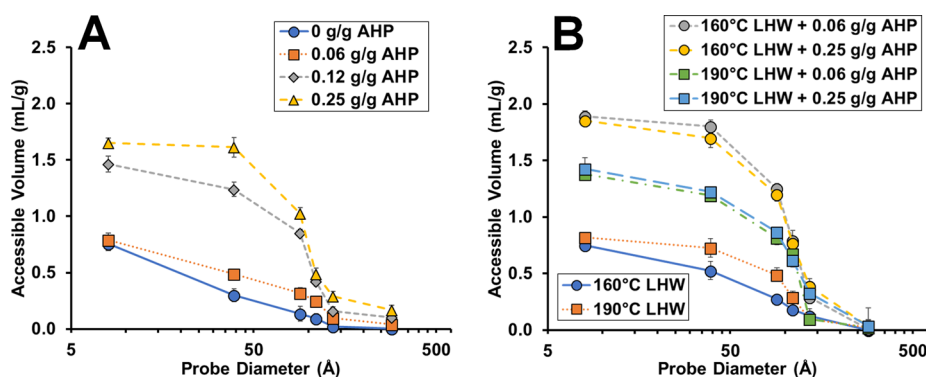


Figure 4. Accessible volume distributions measured by solute exclusion. Accessible volumes of never dried corn stover were determined using neutral dextran probes of average molecular weight range (see Table 1), giving a range of effective hydrodynamic radiuses. (A) AHP-only pretreatment conditions and (B) LHW and the two-stage pretreatments are shown on the right figure. Samples were performed in technical triplicate ($n = 3$), with standard deviation shown in the figure.

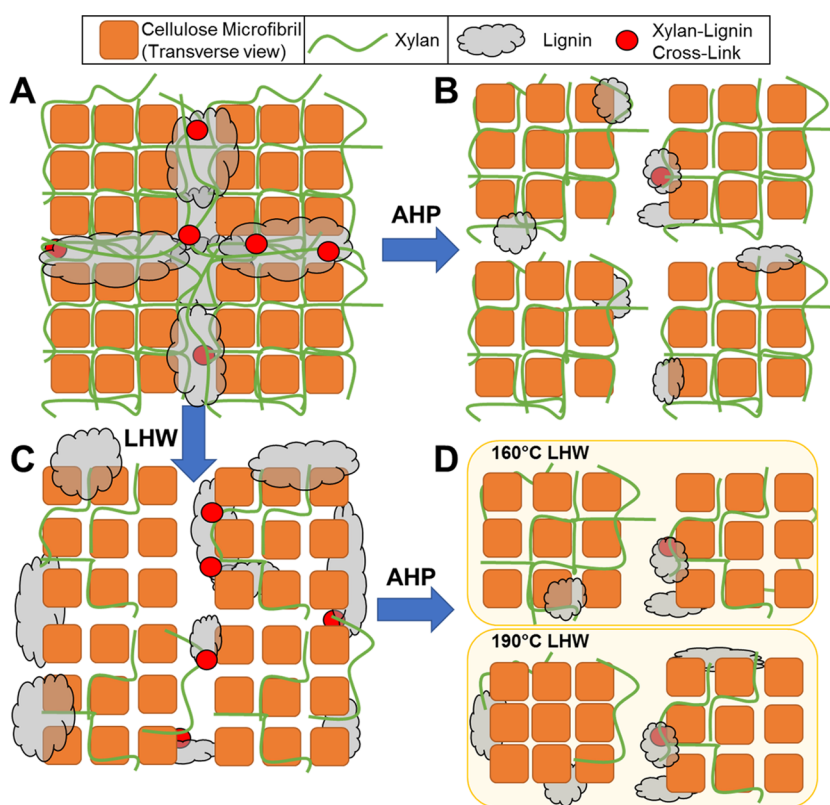


Figure 5. Structural model for pretreatment effect on cell wall organization. Transverse section of cellulose microfibrils for (A) native cell wall, (B) AHP-pretreated cell wall, (C) LHW-pretreated cell wall, and (D) two-stage AHP pretreated LHW cell wall. AHP pretreatment results primarily in reduction of lignin content and cleavage of labile ferulate ester linkages, promoting the formation of porous regions and inducing cell wall swelling. LHW pretreatment primarily removes xylan and relocalizes lignin, increasing accessible surface area. Two-stage pretreatments contain significant reductions in both xylan and lignin content, increasing porous regions, and in the case of 190 °C LHW, sufficient noncellulosic component removal results in cell wall aggregation. Orange squares representing cellulose microfibrils, green lines representing xylan, and gray clouds representing lignin, and red circles representing xylan-lignin cross-links.

39 and 136 Å in the 160 °C LHW and 190 °C LHW condition; however, larger probe volumes were similar to the 0 g/g H_2O_2 AHP-only pretreated sample. In addition, overall accessible volumes were considerably lower compared to AHP-only pretreated samples, indicating limited accessible volume formation in LHW-only samples. One explanation for the limited accessible volumes observed in LHW-only samples may be due melting and relocalization of lignin during pretreatment from spaces between cellulose microfibrils to the cell wall surface⁴¹ together with xylan solubilization that may result in

coalescence of cellulose microfibrils, decreasing the enzyme accessibility of the cellulose (Figure 5C).

For sequential two-stage pretreatment, low H_2O_2 loading coupled with the 160 °C LHW pretreatment condition resulted in accessible volume distributions comparable to the highest H_2O_2 loading for AHP-only pretreatment condition. Increased H_2O_2 loading of the 160 °C LHW condition resulted in higher accessible volumes for the larger probes coupled to minimal increases in smaller probe accessible volumes. This trend was also observed between the low and high H_2O_2 loading for the

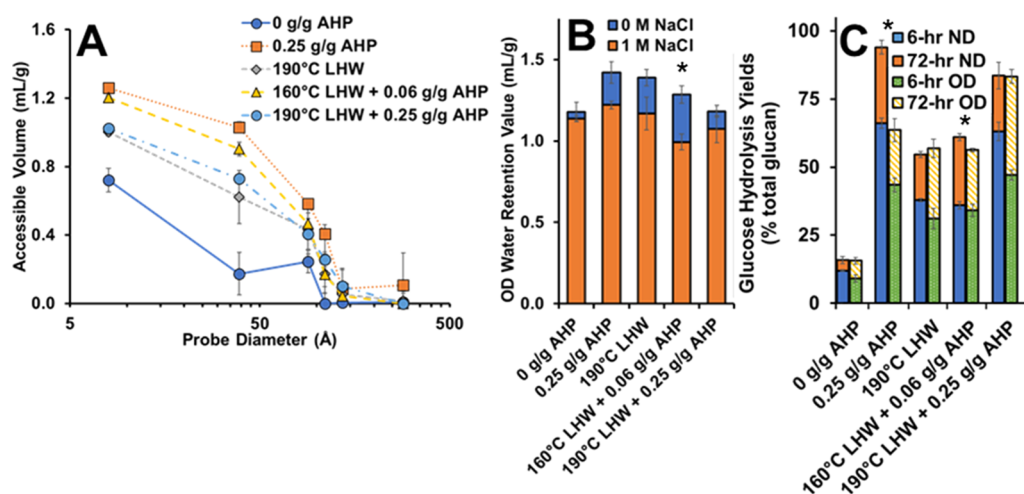


Figure 6. Impact of oven drying on cell wall properties and enzymatic hydrolysis. (A) Accessible volumes of oven-dried and rehydrated corn stover were performed similarly to Figure 4. (B) Water retention value (WRV) of oven-dried corn stover at varying pretreatments. (C) Hydrolysis yields for never-dried (ND) samples with 6-h total hydrolysis time are plotted in blue, and 72-h total hydrolysis time are plotted in orange. Comparative hydrolysis yields for oven-dried (OD) 6-h and 72-h total hydrolysis time from Figure 2 are shown as green dotted and yellow striped bars, respectively. Hydrolysis conditions used 20 mg protein/g glucan CTec3 and 10 mg protein/g glucan HTec3 loading. Experiments were all performed in technical triplicate, with standard deviations shown on each figure. * in (B) indicates statistical significance between 0 M NaCl and 1 M NaCl for individual pretreatment conditions, while * in (C) indicates statistical significance between 72-h OD and 72-h ND yields (Student's *t* test 95% confidence).

190 °C LHW condition, and it likely indicates the formation of larger porous regions with increased H₂O₂ loading rather than the formation of more porous regions in the cell wall as observed in the AHP-only conditions. Smaller probe (<136 Å) accessible volumes were also considerably lower in the 190 °C LHW two-stage pretreatments compared to the 160 °C LHW conditions and support the previously proposed mechanism of either a collapse of interlamellar layers within the cell wall at high overall pretreatment severity, or through cellulose aggregation reducing cell wall porosity due to the lack of xylan to act as a spacer.³⁰ On the basis of results from enzymatic hydrolysis, WRV, and solute exclusion, the following model (Figure 5) was derived for cell wall changes resulting from pretreatment. Figure 5 displays compositional changes resulting from pretreatment in the form of xylan and lignin abundance and location within the cell wall, as well as xylan-lignin ferulate ester cross-links abundance. Structural changes to the secondary cell wall are reflected by increases in fibril bundle spacing demonstrating interlamellar nanoscale porosity and intralamellar microfibril spacing, with both reflecting nanoscale porosity and accessible surface areas.

Impact of Drying-Induced Pore Collapse on Cell Wall Properties and Enzymatic Hydrolysis. Drying-induced hornification was investigated for select pretreatment conditions to determine the impact that changes in higher-order structure of pretreatment-modified cell walls have on cell wall swelling, accessible volumes, and enzymatic hydrolysis yields in compositionally diverse samples. The results show that oven-drying resulted in significant changes in accessible volume distributions (Figure 6A), with decreases in accessible volume observed to some extent for all samples relative to the never-dried samples. There was, however, a stark contrast in how significantly accessible volumes decreased, with samples subjected to AHP delignification demonstrating highly altered accessible volumes, compared to 0 g H₂O₂/g biomass AHP and 190 °C LHW only pretreated biomass, which demonstrated only minimal loss of accessible volumes.⁴² Furthermore, there

was a noted decrease in volumes accessible to larger probes in samples subjected to AHP delignification. These results can be related to the structural model presented in Figure 5, with drying resulting in the collapse of larger porous regions within the cell wall (Figure 5B), while samples containing higher fractions of lignin (Figure 5C) maintained their ability to sorb water within nanoscale pores.⁴³

WRVs were also observed to substantially decrease (Figure 6B), with all samples experiencing at least a 40% decrease in WRV after drying and exhibited a closer distribution of WRV between pretreated biomass compared to the never-dried WRV. Hornification has been demonstrated to reduce accessible internal surface area within delignified wood fibers that limits water sorption.^{44,45} This can be visualized in Figure 5D, with oven-drying removing water and resulting in the irreversible coalescence of some cell wall components.⁴⁶ For the enzymatic hydrolysis yields after oven-drying, the biomass delignified at high H₂O₂ loadings demonstrated the largest decrease in 6-h hydrolysis yields (Figure 6C), followed by less significant decreases for the other pretreated samples. The 72-h hydrolysis yields were only significantly lower in the 0.25 g/g H₂O₂ AHP-only pretreated biomass. As the AHP-delignified biomass is the sample most impacted by drying-induced hornification, this indicates that the hydrated spaces within the cell wall of these samples, presumably containing mostly xylan, are most susceptible to irreversible coalescence. Interestingly, prior work using 0.50 g/g H₂O₂ AHP-delignification followed by lyophilization resulted in no differences in final hydrolysis yields.³² Different methods of drying have been shown to influence extent of hornification and have been explored in the context of altered cell wall properties.⁴⁷

Enzyme Binding. As noted earlier, the commercial cellulase cocktail contains a number of accessory enzyme activities other than cellulase. As a result, the observed bound protein curves represent general protein binding rather than for binding of a specific cellulase. In addition, contributions from cell wall biopolymers other than cellulose (i.e., hemicellulose and lignin)

can contribute to the observed adsorption behavior through nonspecific or nonproductive binding.⁴⁸ However, binding isotherms are useful for assessing the impact of pretreatment on enzyme-accessible surfaces. The results in Figure 7 show the

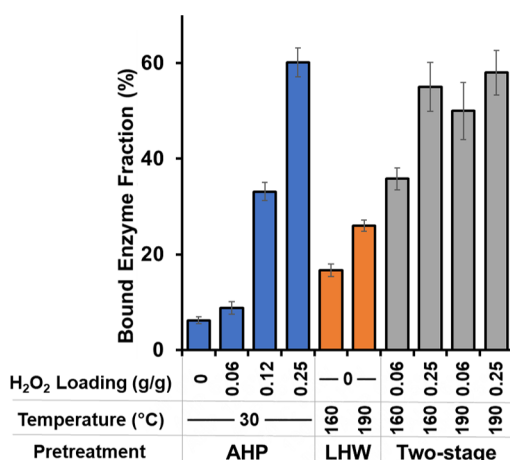


Figure 7. Bound enzyme fractions of CTec3 on pretreated biomass. Bound enzyme fractions are shown as a percent of bound enzyme to total enzyme loading. Binding concentrations were performed in technical duplicate, with the slope of the binding curve determined using linear regression. Error associated with regression fit is shown in the figure.

percent of bound enzyme measured as a fraction of total enzyme in solution for a linear range of enzyme loadings representing the linear, low-concentration region of the binding isotherm. The percentage of bound enzyme increased with increasing H₂O₂ loading for AHP-only pretreated biomass, comparable to results published in our prior work.¹² The LHW-only pretreated biomass had a lower percentage of bound enzyme compared to the higher severity AHP-only pretreated

biomass, indicating that structural changes induced by LHW pretreatment alone do not impact enzyme adsorption the same extent as AHP-delignification. The two-stage pretreatments showed increases in the fraction of bound enzyme with both H₂O₂ loading and to a lesser extent with LHW pretreatment severity; however, low H₂O₂ loadings were still comparable or higher than all but the highest H₂O₂ loading AHP-only pretreated biomass.

Correlation of Properties. By correlating compositional and structural properties of pretreatment-modified plant cell walls to hydrolysis yields, a number of important trends can be identified that provide insight into cell wall matrix changes. The first major trend that can be observed is that comparing 72-h glucose hydrolysis yields to lignin content (Figure 8A) shows three distinct linear relationships between AHP-only and each LHW condition. From this, lignin content can be shown to be correlated with hydrolysis in the context of increased H₂O₂ loading, and therefore, extent of delignification resulting in increased enzymatic hydrolysis yields. The other major compositional difference between each grouping in Figure 8A is the amount of xylan present (shown as a range for each grouping on Figure 8A), which can be taken as a proxy for the extent of cell wall modification during LHW pretreatment.

Next it was observed that glucose hydrolysis yields were positively correlated with 90 Å probe accessible volumes (Figure 8B). Cell wall volumes accessible to the 90 Å dextran probe were selected to correlate with hydrolysis yields, as 90 Å corresponds to a slightly larger probe size than necessary for reasonable estimation of typical cellulase (e.g., TrCel7A).⁴⁹ Notably, as the accessible volumes increased, the 72-h hydrolysis yields were observed to approach saturation. This trend is reasonable, because although accessible volumes may indicate increased accessibility within the cell wall for cellulases, there is likely a limit to the extent accessibility plays in increased enzymatic hydrolysis relative to other intrinsic factors.⁵⁰ Interestingly, for this data set the accessible volumes

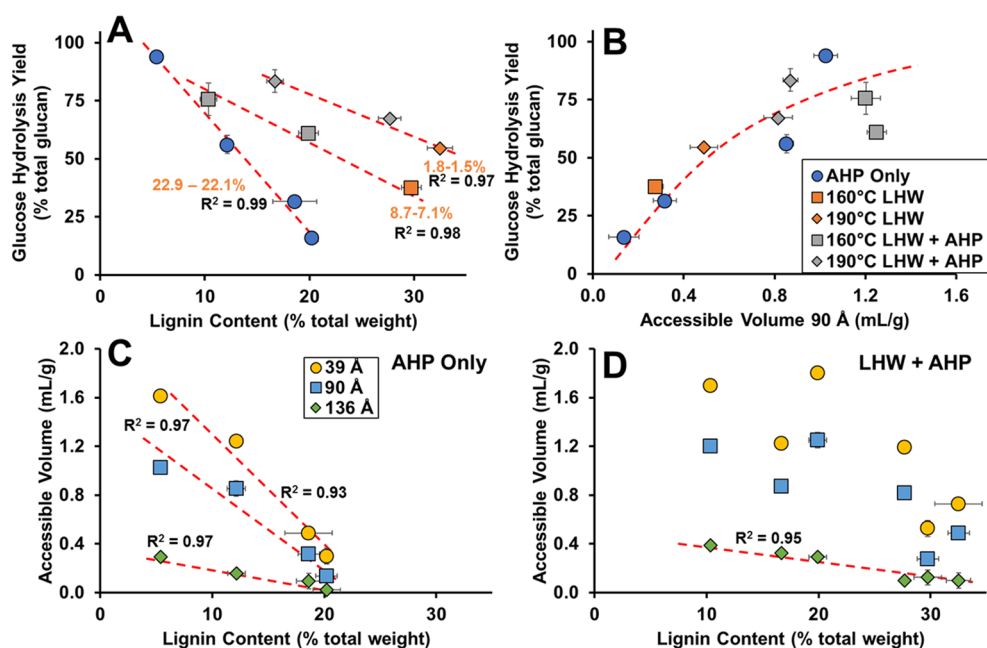


Figure 8. Comparisons between glucose hydrolysis yields, solute exclusion, and lignin content. Glucose hydrolysis yields taken from Figure 2A,B were from 72-h total hydrolysis time using an enzyme solution of CTec3 and HTec3. Xylan content is displayed as a range for each linear trend in orange in panel A. Accessible volume distributions (C,D) were used from Figure 4, and lignin content was taken from Figure 1.

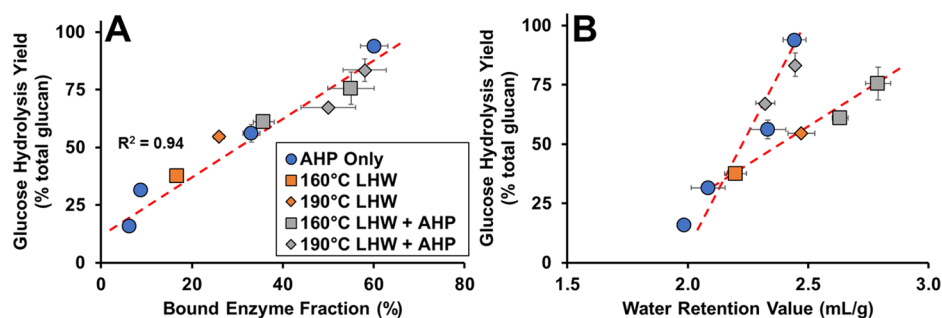


Figure 9. Comparisons between glucose hydrolysis yields and (A) bound enzyme fractions and (B) water retention value. Glucose hydrolysis yields taken from Figure 2 were from 72-h total hydrolysis time using an enzyme solution of CTec3 and HTec3. WRV were taken from Figure 3, and bound enzyme fractions were taken from Figure 7.

across multiple probe sizes were shown to directly correlate to lignin content, with AHP-delignified biomass exhibiting a strong negative correlation with accessible volumes at 39, 90, and 136 Å probe sizes (Figure 8C), while LHW-only and two-stage pretreated biomass accessible volumes correlated only to the 136 Å probe size (Figure 8D). These correlations indicate that for biomass subjected to AHP delignification, increases in the nanoscale probe-accessible volumes can be directly related to the extent of delignification as proposed in the schematic in Figure 5B. Accessible volumes observed in AHP-delignified biomass also likely contribute to enzyme penetration within the cell wall, with prior correlations between enzyme binding and accessible pore volumes shown in sulfite-pretreated hardwoods⁵⁰ and alkali-delignified hardwoods.⁵¹

The fraction of bound enzyme was demonstrated to exhibit a strong positive correlation to glucose hydrolysis yields irrespective of pretreatment conditions or composition (Figure 9A). This result is not surprising as cellulase binding and glucose hydrolysis yields are well-known to be correlated in diverse feedstocks subjected to diverse compositional changes resulting from pretreatment.^{12,33} Correlation plots of WRV versus 72-h hydrolysis yields two distinct trends (Figure 9B), with the AHP-only pretreatment resulting in a clear linear trend between WRV and hydrolysis yields as demonstrated in our prior work,^{12,35} while a second trend with a different slope was observed for the two-stage 160 °C LHW-pretreated biomass. No trend was observed for the two-stage 190 °C LHW-pretreated biomass followed by AHP delignification (Figure 9B), and based upon these results, there appears to be some relationship between glucose hydrolysis yields with water-accessible surface area in pretreated biomass not exhibiting cell wall coalescence due to significant noncellulosic component removal. In addition, these distinct, pretreatment-dependent trends are comparable to what we identified in our prior work with AFEX-pretreated corn stover or switchgrass exhibiting distinct trends for at different ammonia loadings.³⁵

As a final correlation between properties, WRV has also been proposed as a proxy for measuring fiber saturation point (FSP),⁵² which is generally defined as the total inaccessible volume at 560 Å.¹⁶ Additionally, WRV and FSP are hypothesized to measure similar properties in pulps.⁵³ Linear comparisons between the WRVs and FSPs for never-dried and oven-dried pretreated biomass measured show distinct linear trends (Figure 10). In the never-dried samples, the slope of the linear relationship was less than one, indicating WRV measurements were higher than the equivalent inaccessible volume measurement. This is important, because one of the limitations of the solute exclusion method resides in the

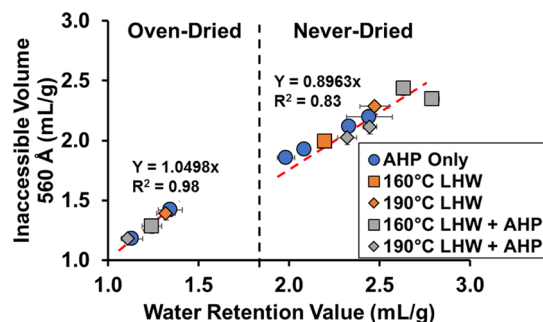


Figure 10. Comparison of inaccessible pore volume to water retention value. Total inaccessible pore volume was determined using solute exclusion at the effective pore size of 560 Å and compared to WRV (0 M NaCl) from Figure 3.

inability for water in porous regions with nonuniform or narrow openings to interact with the dextran probes during the solute-exclusion technique,¹⁸ while WRV accounts for water localized within porous regions of irregular geometries.²⁶ After oven drying, the slope between inaccessible volume and WRV was effectively unity, indicating that the solute exclusion and WRV techniques quantify similar cell wall properties after oven drying. The substantial drop in these properties is clearly attributed to hornification, resulting in the collapse of certain cell wall porous regions and reductions in accessible surfaces shown previously (Figure 6). Based upon this comparison, WRV likely overmeasures total accessible surface area compared to the FSP in the never-dried case, which may be due to WRV also incorporating water–cell wall binding in the form of intralamellar water association within cellulose microfibrils or between microfibrils not be quantified by the FSP. Based upon the two-stage LHW pretreated biomass exhibiting higher WRV relative to FSP (Figure 10) compared to the AHP-delignified only biomass, this may be an appropriate evaluation, as xylan removal could increase water–cellulose microfibril interactions,⁵⁴ while still being inaccessible to quantification by the solute exclusion method. The results and correlations presented in this study provide an avenue of feedstock tailoring within grasses to promote cell wall nanoscale properties conducive to improved enzymatic hydrolysis yields. Specifically, increases in accessible nanoscale surfaces promote high enzymatic hydrolysis yields and depend primarily on cell wall changes induced by AHP pretreatment (Figure 5). It is reasonable to hypothesize that other pretreatments resulting in similar cell wall properties such as increased nanoscale accessible volumes, WRV, and cell wall swelling would also demonstrate high enzymatic hydrolysis

yields comparable to the 0.25 g/g H₂O₂ AHP-only pretreatment.

In summary, AHP delignification and LHW pretreatment of corn stover in this study yielded a series of compositionally diverse feedstocks exhibiting significantly different cell wall properties, that were used to assess how both compositional and structural features impact cell wall recalcitrance to enzymatic hydrolysis. Specifically, we were clearly able to demonstrate that, while the mechanisms by which AHP and LHW pretreatment improve cellulose accessibility are dramatically different, both pretreatment types were shown to increase hydrolysis yields, enzyme sorption, and WRV. AHP delignification was shown to result in a substantial increase in accessible volumes to a series of dextran probes, while LHW pretreatment resulted in only changes to smaller accessible probe distributions. Solute-induced cell wall swelling measured by WRV showed AHP-delignified pretreatments displayed partial loss of cell wall rigidity, which may explain in part larger accessible volume distributions and increased porosity in AHP-delignified biomass. Overall, this study highlights the importance that cell wall organization and modification during processing during biorefining processing can have on feedstock response to enzymatic hydrolysis.

AUTHOR INFORMATION

Corresponding Author

*E-mail: hodgeda@msu.edu.

ORCID

David B. Hodge: [0000-0002-9313-941X](https://orcid.org/0000-0002-9313-941X)

Notes

The authors declare no competing financial interest.

ACKNOWLEDGMENTS

J.C. was supported in part by a grant from NSF (NSF CBET 1336622). R.Z. was supported by the Michigan State University Honor's College. The authors would like to thank Dr. Ryan Stoklosa (USDA-ARS Eastern Regional Research Center, Wyndmoor, PA) for critical review of the manuscript.

REFERENCES

- (1) Himmel, M. E.; Ding, S. Y.; Johnson, D. K.; Adney, W. S.; Nimlos, M. R.; Brady, J. W.; Foust, T. D. Biomass recalcitrance: Engineering plants and enzymes for biofuels production. *Science* **2007**, *315* (5813), 804–807.
- (2) Ding, S.-Y.; Liu, Y.-S.; Zeng, Y.; Himmel, M. E.; Baker, J. O.; Bayer, E. A. How does plant cell wall nanoscale architecture correlate with enzymatic digestibility? *Science* **2012**, *338* (6110), 1055–1060.
- (3) Pauly, M.; Gille, S.; Liu, L.; Mansoori, N.; de Souza, A.; Schultink, A.; Xiong, G. Hemicellulose biosynthesis. *Planta* **2013**, *238* (4), 627–642.
- (4) Vanholme, R.; Demedts, B.; Morreel, K.; Ralph, J.; Boerjan, W. Lignin biosynthesis and structure. *Plant Physiol.* **2010**, *153* (3), 895–905.
- (5) Ralph, J. Hydroxycinnamates in lignification. *Phytochem. Rev.* **2010**, *9* (1), 65–83.
- (6) Crowe, J. D.; Feringa, N.; Pattathil, S.; Merritt, B.; Foster, C.; Dines, D.; Ong, R. G.; Hodge, D. B. Identification of development state and anatomical fraction contributions to cell wall recalcitrance in switchgrass. *Biotechnol. Biofuels* **2017**, *10* (1), 184.
- (7) Ong, R. G.; Chundawat, S. P. S.; Hodge, D. B.; Keskar, S.; Dale, B. E. Linking Plant Biology and Pretreatment: Understanding the Structure and Organization of the Plant Cell Wall and Interactions with Cellulosic Biofuel Production. In *Plants and BioEnergy*; McCann,

M. C., Buckeridge, M. S., Carpita, N. C., Eds.; Springer: New York, 2014; pp 231–253.

- (8) Jeoh, T.; Ishizawa, C. I.; Davis, M. F.; Himmel, M. E.; Adney, W. S.; Johnson, D. K. Cellulase digestibility of pretreated biomass is limited by cellulose accessibility. *Biotechnol. Bioeng.* **2007**, *98* (1), 112–22.

- (9) Zhao, X.; Zhang, L.; Liu, D. Biomass recalcitrance. Part I: the chemical compositions and physical structures affecting the enzymatic hydrolysis of lignocellulose. *Biofuels, Bioprod. Biorefin.* **2012**, *6* (4), 465–482.

- (10) Li, M.; Foster, C.; Kelkar, S.; Pu, Y.; Holmes, D.; Ragauskas, A.; Saffron, C.; Hodge, D. Structural characterization of alkaline hydrogen peroxide pretreated grasses exhibiting diverse lignin phenotypes. *Biotechnol. Biofuels* **2012**, *5* (1), 38.

- (11) Leu, S.-Y.; Zhu, J. Y. Substrate-related factors affecting enzymatic saccharification of lignocelluloses: Our recent understanding. *BioEnergy Res.* **2013**, *6* (2), 405–415.

- (12) Williams, D.; Hodge, D. Impacts of delignification and hot water pretreatment on the water induced cell wall swelling behavior of grasses and its relation to cellulolytic enzyme hydrolysis and binding. *Cellulose* **2014**, *21* (1), 221–235.

- (13) Chandra, R.; Ewanick, S.; Hsieh, C.; Saddler, J. N. The characterization of pretreated lignocellulosic substrates prior to enzymatic hydrolysis, Part I: A modified Simons' staining technique. *Biotechnol. Prog.* **2008**, *24* (5), 1178–1185.

- (14) Liu, H.; Zhu, J. Y.; Chai, X. S. In situ, rapid, and temporally resolved measurements of cellulase adsorption onto lignocellulosic substrates by UV-vis spectrophotometry. *Langmuir* **2011**, *27* (1), 272–8.

- (15) Weiss, N. D.; Thygesen, L. G.; Felby, C.; Roslander, C.; Gourlay, K. Biomass-water interactions correlate to recalcitrance and are intensified by pretreatment: An investigation of water constraint and retention in pretreated spruce using low field NMR and water retention value techniques. *Biotechnol. Prog.* **2017**, *33*, 146–153.

- (16) Stone, J. E.; Scallan, A. M. A structural model for the cell wall of water swollen wood pulp fibres based on their accessibility to macromolecules. *Cellul Chem. Technol.* **1968**, *2*, 343–358.

- (17) Stone, J. E.; Scallan, A. M. The Effect of Component Removal Upon the Porous Structure of the Cell Wall of Wood. *Pulp Pap Mag Can.* **1968**, *69* (12), 69–74.

- (18) Beecher, J. F.; Hunt, C. G.; Zhu, J. Y. Tools for the Characterization of Biomass at the Nanometer Scale. In *The Nanoscience and Technology of Renewable Biomaterials*; Lucia, L. A., Rojas, O., Eds.; John Wiley & Sons, Ltd: Hoboken, NJ, 2009; pp 61–90.

- (19) Park, S.; Venditti, R. A.; Jameel, H.; Pawlak, J. J. Changes in pore size distribution during the drying of cellulose fibers as measured by differential scanning calorimetry. *Carbohydr. Polym.* **2006**, *66* (1), 97–103.

- (20) Ishizawa, C. I.; Davis, M. F.; Schell, D. F.; Johnson, D. K. Porosity and Its Effect on the Digestibility of Dilute Sulfuric Acid Pretreated Corn Stover. *J. Agric. Food Chem.* **2007**, *55* (7), 2575–2581.

- (21) Grethlein, H. E. The effect of pore-size distribution on the rate of enzymatic-hydrolysis of cellulosic substrates. *Bio/Technology* **1985**, *3* (2), 155–160.

- (22) Junior, C. S.; Milagres, A. M. F.; Ferraz, A.; Carvalho, W. The effects of lignin removal and drying on the porosity and enzymatic hydrolysis of sugarcane bagasse. *Cellulose* **2013**, *20* (6), 3165–3177.

- (23) Pihlajaniemi, V.; Sipponen, M. H.; Liimatainen, H.; Sirviö, J. A.; Nyyssölä, A.; Laakso, S. Weighing the factors behind enzymatic hydrolyzability of pretreated lignocellulose. *Green Chem.* **2016**, *18* (5), 1295–1305.

- (24) Foster, C. E.; Martin, T. M.; Pauly, M., Comprehensive compositional analysis of plant cell walls (lignocellulosic biomass) part II: carbohydrates. *J. Visualized Exp.* **2010**, (37), DOI: [10.3791/1745](https://doi.org/10.3791/1745)

- (25) Sluiter, J. B.; Ruiz, R. O.; Scarlata, C. J.; Sluiter, A. D.; Templeton, D. W. Compositional Analysis of Lignocellulosic Feedstocks. 1. Review and Description of Methods. *J. Agric. Food Chem.* **2010**, *58* (16), 9043–9053.

- (26) Stone, J. E.; Scallan, A. M. The Effect of Component Removal Upon Porous Structure of Cell Wall of Wood: Swelling in Water and Fiber Saturation Point. *TAPPI J.* **1967**, *50*, 496–501.
- (27) Bradford, M. M. A rapid and sensitive method for the quantitation of microgram quantities of protein utilizing the principle of protein-dye binding. *Anal. Biochem.* **1976**, *72* (1–2), 248–254.
- (28) Banerjee, G.; Car, S.; Liu, T. J.; Williams, D. L.; Meza, S. L.; Walton, J. D.; Hodge, D. B. Scale-up and integration of alkaline hydrogen peroxide pretreatment, enzymatic hydrolysis, and ethanolic fermentation. *Biotechnol. Bioeng.* **2012**, *109* (4), 922–931.
- (29) Mosier, N.; Hendrickson, R.; Ho, N.; Sedlak, M.; Ladisch, M. R. Optimization of pH controlled liquid hot water pretreatment of corn stover. *Bioresour. Technol.* **2005**, *96* (18), 1986–1993.
- (30) Ishizawa, C. I.; Jeoh, T.; Adney, W. S.; Himmel, M. E.; Johnson, D. K.; Davis, M. F. Can delignification decrease cellulose digestibility in acid pretreated corn stover? *Cellulose* **2009**, *16*, 677–686.
- (31) Sun, F. F.; Hong, J.; Hu, J.; Saddler, J. N.; Fang, X.; Zhang, Z.; Shen, S. Accessory enzymes influence cellulase hydrolysis of the model substrate and the realistic lignocellulosic biomass. *Enzyme Microb. Technol.* **2015**, *79–80*, 42–48.
- (32) Banerjee, G.; Car, S.; Scott-Craig, J. S.; Hodge, D. B.; Walton, J. D. Alkaline peroxide pretreatment of corn stover: effects of biomass, peroxide, and enzyme loading and composition on yields of glucose and xylose. *Biotechnol. Biofuels* **2011**, *4* (1), 16.
- (33) Kumar, R.; Wyman, C. E. Cellulase adsorption and relationship to reatures of corn stover solids sroduced by leading pretreatments. *Biotechnol. Bioeng.* **2009**, *103* (2), 252–267.
- (34) Lu, Y. P.; Yang, B.; Gregg, D.; Saddler, J. N.; Mansfield, S. D. Cellulase adsorption and an evaluation of enzyme recycle during hydrolysis of steam-exploded softwood residues. *Appl. Biochem. Biotechnol.* **2002**, *98*, 641–654.
- (35) Williams, D. L.; Crowe, J. D.; Ong, R. G.; Hodge, D. B. Water sorption in AFEX- and AHP-pretreated grasses as a predictor of enzymatic hydrolysis yields. *Bioresour. Technol.* **2017**, DOI: [10.1016/j.biortech.2017.08.200](https://doi.org/10.1016/j.biortech.2017.08.200)
- (36) Grignon, J.; Scallan, A. M. Effect of pH and neutral salts upon the swelling of cellulose gels. *J. Appl. Polym. Sci.* **1980**, *25* (12), 2829–2843.
- (37) Boerjan, W.; Ralph, J.; Baucher, M. Lignin biosynthesis. *Annu. Rev. Plant Biol.* **2003**, *54*, 519–546.
- (38) Okay, O. General properties of hydrogels. In *Hydrogel sensors and actuators*; Gerlach, G., Arndt, K.-F., Eds.; Springer: Berlin, 2009; pp 1–14.
- (39) Carlsson, G.; Kolseth, P.; Lindstrom, T. Polyelectrolyte swelling behavior of chlorite delignified spruce wood fibers. *Wood Sci. Technol.* **1983**, *17* (1), 69–73.
- (40) Grethlein, H. E. The effect of pore-size distribution on the Rate of Enzymatic Hydrolysis of Cellulosic Substrates. *Bio/Technology* **1985**, *3* (2), 155–160.
- (41) Selig, M. J.; Viamajala, S.; Decker, S. R.; Tucker, M. P.; Himmel, M. E.; Vinzant, T. B. Deposition of lignin droplets produced during dilute acid pretreatment of maize stems retards enzymatic hydrolysis of cellulose. *Biotechnol. Prog.* **2007**, *23* (6), 1333–1339.
- (42) Stone, J. E.; Treiber, E.; Abrahamson, B. Accessibility of Regenerated Cellulose to Solute Molecules. *TAPPI J.* **1969**, 108–110.
- (43) Fernandes Diniz, J. M. B.; Gil, M. H.; Castro, J. A. A. M. Hornification—its origin and interpretation in wood pulps. *Wood Sci. Technol.* **2004**, *37* (6), 489–494.
- (44) Luo, X. L.; Zhu, J. Y.; Gleisner, R.; Zhan, H. Y. Effects of wet-pressing-induced fiber hornification on enzymatic saccharification of lignocelluloses. *Cellulose* **2011**, *18* (4), 1055–1062.
- (45) Luo, X.; Zhu, J. Y. Effects of drying-induced fiber hornification on enzymatic saccharification of lignocelluloses. *Enzyme Microb. Technol.* **2011**, *48* (1), 92–99.
- (46) Pönni, R.; Vuorinen, T.; Kontturi, E. Proposed nano-scale coalescence of cellulose in chemical pulp fibers during technical treatments. *BioResources* **2012**, *7* (4), 6077–6108.
- (47) Wong, K. K.; Deverell, K. F.; Mackie, K. L.; Clark, T. A.; Donaldson, L. A. The relationship between fiber-porosity and cellulose digestibility in steam-exploded *Pinus radiata*. *Biotechnol. Bioeng.* **1988**, *31* (5), 447–456.
- (48) Strobel, K. L.; Pfeiffer, K. A.; Blanch, H. W.; Clark, D. S. Structural insights into the affinity of Cel7A carbohydrate-binding module for lignin. *J. Biol. Chem.* **2015**, *290* (37), 22818–26.
- (49) Wang, Q. Q.; He, Z.; Zhu, Z.; Zhang, Y. H.; Ni, Y.; Luo, X. L.; Zhu, J. Y. Evaluations of cellulose accessibilities of lignocelluloses by solute exclusion and protein adsorption techniques. *Biotechnol. Bioeng.* **2012**, *109* (2), 381–9.
- (50) Mooney, C. A.; Mansfield, S. D.; Touhy, M. G.; Saddler, J. N. The effect of initial pore volume and lignin content on the enzymatic hydrolysis of softwoods. *Bioresour. Technol.* **1998**, *64* (2), 113–119.
- (51) Meng, X.; Wells, T., Jr.; Sun, Q.; Huang, F.; Ragauskas, A. Insights into the effect of dilute acid, hot water or alkaline pretreatment on the cellulose accessible surface area and the overall porosity of *Populus*. *Green Chem.* **2015**, *17* (8), 4239–4246.
- (52) Hui, L.; Liu, Z.; Ni, Y. Characterization of high-yield pulp (HYP) by the solute exclusion technique. *Bioresour. Technol.* **2009**, *100* (24), 6630–6634.
- (53) Scallan, A. M.; Carles, J. E. Correlation of water retention value with fiber saturation point. *Svensk Papperstid-Nord Cellul* **1972**, *75* (17), 699.
- (54) Olsson, A. M.; Salmen, L. The association of water to cellulose and hemicellulose in paper examined by FTIR spectroscopy. *Carbohydr. Res.* **2004**, *339* (4), 813–818.